OncoTargets and Therapy

Dovepress
open access to scientific and medical research

Open Access Full Text Article

ORIGINAL RESEARCH

Near-Infrared Light-Triggered Thermosensitive Liposomes Modified with Membrane Peptides for the Local Chemo/Photothermal Therapy of Melanoma

This article was published in the following Dove Press journal:
OncoTargets and Therapy

Xinxin Li[1,2,*]
Chunsheng Yang[3,4,*]
Yingkai Tao[1,2]
Xiaoyang Hou[1,2]
Yanqun Liu[1,2]
Hong Sang[3]
Guan Jiang[1,2]

[1]Department of Clinical Medicine, Xuzhou Medical University, Xuzhou, 221004, People's Republic of China; [2]Department of Dermatology, Affiliated Hospital of Xuzhou Medical University, Xuzhou, 221002, People's Republic of China; [3]Jinling Hospital Department of Dermatology, Nanjing Medical University, Nanjing, 210002, People's Republic of China; [4]Department of Dermatology, The Affiliated Huai'an Hospital of Xuzhou Medical University, The Second People's Hospital of Huai'an, Huai'an, 223002, People's Republic of China

*These authors contributed equally to this work

Purpose: A near-infrared (NIR)-triggered trans-activating transcriptional activator (TAT)-based targeted drug delivery system for the combined chemo/photothermal therapy of melanoma, namely, TAT-TSL-TMZ (temozolomide)/IR820, was developed for the first time.

Methods: TAT-TSL-TMZ/IR820 liposomes were synthesized via thin-film dispersion and sonication. IR820 and TMZ were encased in the inner layer and lipid bilayer of the liposomes, respectively.

Results: Dynamic light scattering results showed that the liposomes had an average hydrodynamic size of 166.9 nm and a zeta potential of −2.55 mV. The encapsulation rates of TMZ and IR820 were 35.4% and 28.6%, respectively. The heating curve obtained under near-infrared (NIR) laser irradiation showed that TAT-TSL-TMZ/IR820 liposomes had good photothermal conversion efficiency. The in vitro drug release curve revealed that NIR laser irradiation could accelerate drug release from TAT-TSL-TMZ/IR820 liposomes. The results of inverted fluorescence microscopy and flow cytometry proved that the uptake of TAT-TSL-TMZ/IR820 liposomes by human melanoma cells (MV3 cells) was concentration-dependent and that the liposomes modified with membrane peptides were more likely to be ingested by cells than unmodified liposomes. Confocal laser scanning microscopy indicated that TAT-TSL-TMZ/IR820 liposomes entered MV3 cells via endocytosis and was stored in lysosomes. In addition, TAT-TSL-TMZ/IR820 liposomes exposed to NIR laser showed 89.73% reduction in cell viability.

Conclusion: This study investigated the photothermal conversion, cell uptake, colocation and chemo/photothermal effect of TAT-TSL-TMZ/IR820 liposomes.

Keywords: melanoma, liposome, TAT, photothermal therapy, temozolomide, IR820

Introduction

Melanoma is a malignant tumor that originates from deep melanocytes in the epidermis and develops through benign dysfunction.[1,2] Although the incidence of many other types of cancer is declining, that of melanoma is continually increasing.[3] Melanoma is an aggressive, fatal, unpredictable skin tumor that tends to affect younger people.[4] Chemotherapy plays a crucial role in melanoma treatment. Temozolomide (TMZ) is a novel antitumor alkylating agent that is similar to dacarbazine (DTIC), a clinically administered oral drug. TMZ is highly bioavailable, well-tolerated by patients, and widely distributed in tissues. Moreover, it can cross the blood–brain barrier, and it improves the quality of life of patients with metastatic melanoma. Hence, many countries recommend TMZ as an oral

Correspondence: Hong Sang
Jinling Hospital Department of Dermatology, Nanjing Medical University, Nanjing, 210002, People's Republic of China
Email sanghong@nju.edu.cn

Guan Jiang
Department of Clinical Medicine, Xuzhou Medical University, Xuzhou, 221004, People's Republic of China
Email dr.guanjiang@xzhmu.edu.cn

submit your manuscript | www.dovepress.com
DovePress
http://doi.org/10.2147/OTT.S287272

alternative to DTIC. However, TMZ has limited therapeutic efficacy in melanoma because of drug resistance and instability. Thus, developing an effective drug delivery system for improving the sensitivity of chemotherapy has attracted increasing research attention.

Drug delivery systems based on nanotechnology have caught the attention of scholars. In recent years, great progress has been made in the development of nanoparticles for use as smart devices for diagnostics and targeted therapeutics.[5] Nanoparticles have unique biological structures and physicochemical properties, such as their nanoscale size, surface effect, good biocompatibility, multifunctional effect, and optical and magnetic properties.[6] Many nanoscale drug delivery systems (NDDSs) for prolonging the circulation time of chemotherapeutics and maximizing their tumor uptake via the enhanced permeability and retention (EPR) effect and/or active targeting mechanisms have been rationally designed. Moreover, NDDSs promise to alleviate the severe systemic or organ-specific toxicities of anticancer drugs.[7] Nanoparticles exhibit passive targeting and slow release and can thus be used as carriers to deliver drugs specifically to target sites, achieve continuous drug release in tumors, effectively prolong the half-life of drugs, and reduce the cytotoxicity of drugs to normal tissues. Early clinical trials have demonstrated that polymer-drug conjugates have several advantages, including enhanced antitumor efficacy, reduced side effects, facile drug administration, and improved patient compliance and long-term prognosis, over their corresponding antitumor drugs.[8] Although the use of nanodelivery systems loaded with chemotherapeutic drugs have made great progress in antitumor therapy in recent years, the single treatment model is not ideal. Photothermal therapy (PTT) is a new and effective tumor treatment technology wherein near-infrared (NIR) dye is used to mediate the conversion of near-infrared (NIR) light into heat energy to inflict irreversible damage to tumor tissues. PTT has unique advantages, such as increased specificity and reduced invasiveness and adverse reactions, over traditional therapy.[9] Indocyanine green (ICG) is the only NIR dye that has been approved by the US Food and Drug Authority that can improve local temperature and perform photothermal functions after NIR irradiation.[10,11] IR820 is a derivative of ICG with a similar structure and performance as ICG. It has a molecular structure of $C_{46}H_{50}ClN_2NaO_6S_2$. This molecule is water-soluble and can be encapsulated within the inner cavities of liposomes. IR820 is more stable at different temperatures and has longer tissue retention time and better biosecurity than ICG.[12] PTT can kill primary tumor cells but cannot eradicate metastatic tumor cells, whereas chemotherapy, as a systemic treatment, can kill primary and metastatic tumor cells.[13] Therefore, the combination of chemotherapy and PTT in the treatment of cancer has attracted considerable attention in basic research and clinical practice.[14–16]

Over the past few decades, scholars have studied many nanodrug delivery carriers, including liposomes, polymeric micelles, polymer-drug conjugates, and dendritic macromolecular nucleic acid nanoparticles, among which liposomes and polymer-drug conjugates are the dominant nanoparticles in clinical applications.[17] A unique feature of liposomes is that they can encapsulate a variety of lipophilic and hydrophilic substances. Hydrophilic molecules are encapsulated in the internal water phase, whereas hydrophobic molecules are contained in the lipid bilayer. The phospholipid membranes of thermosensitive liposomes are characterized by their sensitivity to temperature. The liposome membrane changes from the colloidal state into the liquid crystal state at temperatures above the phase transition temperature; this change results in the release of a large amount of drugs by increasing the permeability of the liposome bilayer membrane.[18] The introduction of cholesterol into liposomes can improve serum stability.[19] Polyethylene glycol (PEG) can extend the blood circulation time of liposomes, reduce the clearance of liposomes by the reticuloendothelial system, and prevent the nonspecific biological distribution of drugs.[20,21] Dipalmitoyl phosphatidylcholine (DPPC), a major component of thermosensitive liposomes, has the properties and biocompatibility of mature vesicles. DPPC can be transformed into a liquid crystal when the local hyperthermia temperature is slightly higher than the body temperature (41.5 °C –41.9 °C) and is thus a good liposome candidate for the hyperthermia-induced controlled release of drugs.[22]

Drug delivery to the targeted cell is useful for the pharmacological action of most anticancer drugs. Cell membrane-penetrating peptides, which are short peptides that are composed of 10–30 amino acids with special functions, are expected to overcome the obstacles of drug delivery in cells. Trans-activating transcriptional activators (TATs) are one of the most commonly used membrane peptides in cells and have been successfully used to transport all kinds of materials, such as small particles, proteins, and even drugs, in vivo and in vitro without remarkable side effects on host

cells.[23] TAT ligands can improve cell penetration efficiency through nonspecific endocytosis.[24]

In this study, a NIR-triggered TAT-based targeted drug delivery system for the combined chemo/photothermal therapy of melanoma, namely, TAT-TSL-TMZ/IR820, was developed for the first time via self-assembly. First, liposomes containing TMZ and IR820-modified TAT were prepared. Subsequently, the particle size, morphology, heating capacity, and drug release capacity of the liposomes were measured. Finally, the uptake and intracellular distribution of TAT-TSL-TMZ/IR820 liposomes in human melanoma cells (MV3 cells) were detected in vitro. In addition, the results of CCK8 indicated that TAT-TSL-TMZ/IR820 liposomes had chemo/photothermal effect.

Materials and Methods

Materials

DPPC was purchased from Avanti Polar Lipids Co. Ltd. DSPE-PEG2000 and DSPE-PEG2000-Mal were purchased from Xian Ruixi Biotechnology Co., Ltd. TAT peptide with terminal cysteine (Cys-AYGRKKRRQRRR) was synthesized by GL Biochem Co., Ltd. (Shanghai, China). IR820 was purchased from Sigma-Aldrich (Merck KGaA). TMZ was obtained from Tokyo Chemical Industry Co., Ltd. 4-6-Diamidino-2-phenylindole (DAPI) and coumarin 6 were purchased from Beijing Soleboard Biotechnology Co., Ltd. LysoTracker Red was purchased from Shanghai Biyuntian Biotechnology Co., Ltd. Other solvents and reagents were purchased from Beijing Chemical Works.

Synthesis of DSPE-PEG2000-TAT Liposomes

DSPE-PEG2000-TAT was synthesized as described previously.[23,24] Briefly, 20 mg of DSPE-PEG2000-Mal and 15 mg of Cys-TAT were reacted in 5 mL of water with gentle stirring at room temperature for approximately 24 h. The solvent was then dialyzed for 48 h against deionized water by using a membrane with the molecular weight cut-off of 8000–14,000 Da. The product was then lyophilized for further use. An infrared spectrometer was used to characterize and analyze the infrared spectrum of DSPE-PEG2000-TAT liposomes. Appropriate amounts of TAT, DSPE-PEG2000-Mal, and DSPE-PEG2000-TAT liposomes were collected for the KBr tablet test.

Preparation of Liposomes

DPPC, cholesterol, DSPE-PEG2000, and DSPE-PEG2000 -TAT were formulated at the mass ratio of 16:4:1:1 for liposome preparation. Liposomes were passively loaded with TMZ and IR820 for therapeutic application. Briefly, 5 mg of TMZ and 0.5 mg of IR820 along with the lipid mixture were dissolved in methanol and chloroform (volume ratio 1:5) and dried in a round-bottomed flask to form a homogeneous lipid film. Then, an appropriate amount of PBS was added, and ultrasonic hydration was performed to form a uniform suspension. The liposomes were then ultrasonicated with an ultrasonic cell fragmentation apparatus and centrifuged at 10,000 r/min for 20 min by using a high-speed refrigerated centrifuge at 4 °C to remove unencapsulated drugs and free lipids. The suspension precipitate was mixed with PBS and then passed through 220 nm polyethersulfone filters. The final TAT-TSL-TMZ/IR820 liposome solution was thus obtained and stored in a refrigerator at 4 °C.

TSL-TMZ/IR820 liposomes were prepared through the same steps, except that DSPE-PEG2000-TAT liposomes was excluded from the preparation process. Coumarin 6-labeled TAT-TSL-TMZ/IR820 liposomes were prepared, and 1 mg/mL coumarin 6 was added to dimethyl sulfoxide.

Characterization of Liposomes

The hydrodynamic size, polydispersity index (PDI), and zeta potential of the TAT-TSL-TMZ/IR820 liposomes were measured via dynamic light scattering (DLS) by using a Zetasizer apparatus (Zetasizer Nano ZS, Malvern Instruments, Ltd.). The morphology of the liposomes was observed through TEM. One drop of the TAT-TSL-TMZ /IR820 liposomes suspension was dripped onto a special copper grid, dried at room temperature, and observed via TEM.

Encapsulation Efficiency

TMZ and IR820 were used to prepare standard solutions, and standard solutions with different concentrations of TMZ and IR820 were set. The standard solutions were subjected to UV–visible spectroscopy to detect their maximum absorption wavelengths. A standard curve was drawn by measuring the absorbance of the standard at the maximum absorption wavelength.

The unencapsulated drugs were separated from the precipitate via ultraspeed centrifugation at 10,000 r/min for 20 min at 4 °C, and the supernatant was collected and

demulsified after each centrifugation. The centrifuged supernatant was collected and diluted several times, and the absorbance of the diluted supernatant was measured with an UV spectrophotometer. The corresponding standard curve was established on the basis of the concentration of the unencapsulated drug in the supernatant.

The quality of the unencapsulated drug = the concentration × the dilution × the volume.

Encapsulation efficiency = (weight of drug initially added − unencapsulated drug quality)/weight of drug initially added × 100%.

Temperature Increase Curve Under NIR Laser Irradiation

A NIR laser (808 nm, 4 W/cm^2) was used to irradiate the PBS solution (pH 7.4) containing TAT-TSL-TMZ/IR820 liposomes (0, 5, 10, 15, and 20 μg/mL IR820) for 5 min at 25 °C. The temperature increments shown by the TAT-TSL -TMZ/IR820 solution at different time points were recorded by using an infrared thermal imaging camera.

PBS solutions (pH 7.4) with or without free IR820 (20 μg/mL) or TAT-TSL-TMZ/IR820 liposomes (20 μg/mL IR820) were irradiated with a NIR laser at 4 W/cm^2 for 5 min. The temperature was recorded by using an infrared thermal imaging camera and used to construct the temperature increase curve.

Determination of Drug Release in vitro

The release of TMZ from the TAT-TSL-TMZ/IR820 liposomes was studied in PBS (pH 5.4) by using an 8.4–35k dialysis bag. Drug release was measured through the following steps: TAT-TSL-TMZ/IR820 liposome solution (1 mL) was placed into the dialysis bag. The two ends of the dialysis bag were tied tightly with a thin wire, and the drug was released into 20 mL of PBS (pH 5.4). The dialytic release device was kept at 37 °C in a thermostatic oscillator for 30 min. Then, the liposome solution was treated under laser irradiation (4 W/cm^2) for 5 min and placed in the thermostatic oscillator to simulate drug release again. The released liquid (1 mL) was absorbed over a certain time interval. Then, 1 mL of PBS (pH 5.4) was added, and the dialysis bag was placed back into the thermostatic oscillator for further oscillation. The cumulative release amount of the drug in each time period was calculated, and the cumulative release curve was drawn in accordance with the concentration of each sample.

Cell Culture

MV3 cells were acquired from the Type Culture Collection of the Chinese Academy of Science (Shanghai, China). The cells were routinely incubated in Dulbecco's modified Eagle's medium (DMEM) supplemented with 10% fetal bovine serum, 100 U/mL penicillin, and 100 μg/mL streptomycin at 37 °C with 5% CO_2 and saturated humidity.

Cytotoxicity

MV3 cells in the logarithmic growth stage were digested with trypsin. The cells (4×10^4 cells/well) were seeded in 96-well plates and cultured overnight at 37 °C with 5% CO_2. Then, the medium was replaced with a complete medium containing TAT-TSL-TMZ/IR820 liposomes (1, 2, 4, 8, 16, and 32 μg/mL). The control group was continuously cultured in an incubator. CCK-8 solution (10 μL) was added to each well, and the plates were incubated at 37 °C for 2 h. The absorbance of each well was measured at the wavelength of 450 nm with an enzyme marker, and the experimental results were recorded.

Cellular Uptake Analysis

The cellular uptake behavior of TAT-TSL-TMZ/IR820 liposomes at different concentrations was detected through inverted fluorescence microscopy and flow cytometry. MV3 cells were seeded in six-well plates at a density of 2×10^5 cells/well for 24 h. Subsequently, TAT-TSL-TMZ/IR820 liposomes (0, 4, 8, and 16 μg/mL) labeled with coumarin 6 and TSL-TMZ/IR820 liposomes (16 μg/mL) were separately added into the culture medium and coincubated with the cells for 3 h. The medium was aspirated out, and the cells were washed with PBS. Subsequently, the cells were fixed by adding 4% paraformaldehyde at room temperature for 15 min. The cells were stained with DAPI (nucleus, blue color) for 15 min and observed immediately with an inverted fluorescence microscope. Flow cytometry was further performed to measure cell uptake. In brief, MV3 cells were cultured with DMEM in a six-well culture plate for 24 h. Subsequently, TAT-TSL-TMZ/IR820 liposomes (0, 4, 8, and 16 μg/mL) labeled with coumarin 6 and TSL-TMZ/IR820 liposomes (16 μg/mL) were separately added to the medium and coincubated with the cells for 3 h. The cells were washed with PBS, digested with trypsin, and collected through centrifugation (1500 r/min, 5 min). Finally, the cells were resuscitated with PBS and analyzed via flow cytometry.

Intracellular Localization Analysis

Confocal laser scanning microscopy (CLSM) was used to observe the distribution of TAT-TSL-TMZ/IR820 liposomes in MV3 cells. MV3 cells in the logarithmic growth stage were inoculated overnight in a confocal glass plate at a cell density of 1×10^5. TAT-TSL-TMZ /IR820 liposomes (16 μg/mL) were added to the culture medium and coincubated for 3 h. Then, the cells were washed with PBS, treated with 1 mL of LysoTracker Red dye (50 nm) medium, and incubated at 37 °C for 1 h. Finally, the images of liposome distribution were collected immediately through CLSM.

Detection of the Cytotoxicity of TAT-TSL-TMZ/IR820 Liposomes Combined with NIR to MV3 Cells by the Cell Counting Kit 8 Assay

MV3 cells were seeded in 24 well plates at a cell density of 50,000 well and cultured overnight in an incubator.

The following experimental groups were established:

a. Ctr; b. NIR; c. TAT-TSL-TMZ/IR820; d. IR820 +NIR; e.TAT-TSL-TMZ+NIR; f. TAT-TSL-IR820+NIR; and g. TAT-TSL-TMZ/IR820+NIR.

The corresponding drug culture medium was added according to the groups for 24 h at 37°C.The laser group was irradiated with 808 nm NIR of 4 W/cm2 for 5min. After exposure, we returned plates to the incubator for 24h,then cck-8 solution was added to each well in the dark for 2 h at 37°C.The liquid in the corresponding hole was transferred to 96-well plates and detected the optical density (OD) value.

Statistical Analysis

Statistical analyses were performed by using either unpaired Student's *t*-test or one-way ANOVA. $P < 0.05$ was considered as statistically significant.

Results

Synthesis and Characterization of DSPE-PEG2000-TAT Liposomes

The chemical structure of DSPE-PEG2000-TAT liposomes was confirmed through infrared spectrometry. Figure 1 shows that the formation of DSPE-PEG2000-TAT liposomes was accompanied by the disappearance of the DSPE-PEG2000-Mal spot after the reaction. The peak at 2525 cm^{-1} in the spectrum of TAT was the characteristic absorption peak of –SH (Figure 1A). Figure 1B shows that the spectrum of DSPE-PEG2000-Mal lacked interference from the absorption peak at this position, whereas the absorption peak disappeared in the spectrum of DSPE-PEG2000-TAT liposomes. This occurrence indicated that –SH in the TAT peptide had successfully connected with the maleimide group in DSPE-PEG2000-Mal (Figure 1C).

Preparation and Characterization of TAT-TSL-TMZ/IR820 Liposomes

The schematic of the thermosensitive TAT-TSL-TMZ/IR820 liposomes is shown in Figure 2. The liposomes self-assembled from DPPC, cholesterol, DSPE-PEG2000, DSPE-PEG2000-TAT, TMZ, and IR820 through thin-film dispersion and sonication. First, DSPE-PEG2000-TAT was synthesized, and homogenous lipid membranes were then prepared by using the membrane dispersion method. The hydrophilic IR820 was dispersed in the inner layer of the liposomes, and the lipophilic TMZ was dispersed in the lipid

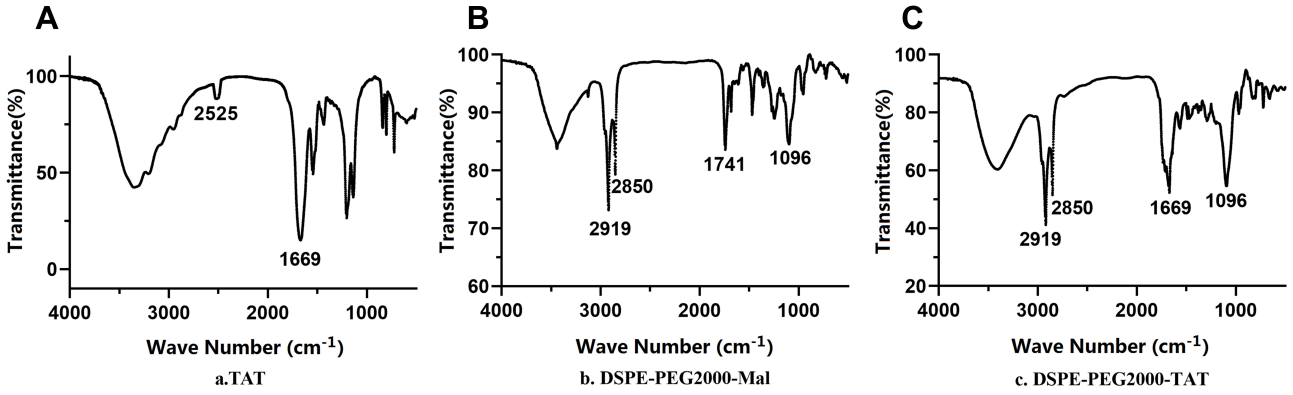

Figure 1 Infrared spectra of (**A**)TAT and (**B**)DSPE-PEG2000-Mal before TAT reaction, (**C**)DSPE-PEG2000-TAT after TAT reaction.

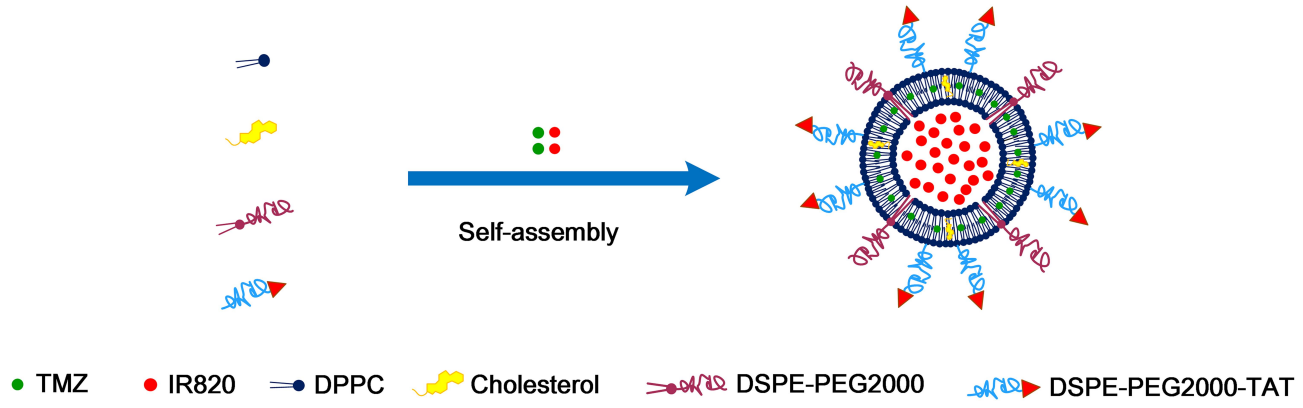

Figure 2 Schematic of the preparation of TAT-TSL-TMZ/IR820 liposomes.

bilayer. The presence of IR820 rendered the lipid shell of the liposomes vulnerable to laser damage and enabled the drug to escape from the nanocarrier effectively. DLS was performed to describe particle size, PDI, and zeta potential. The results are summarized in Figure 3. The liposomes had an average hydrodynamic size of approximately 166.9 nm, a PDI of 0.167, and a zeta potential of −2.55 mV. The particle size results suggested that the liposomes could

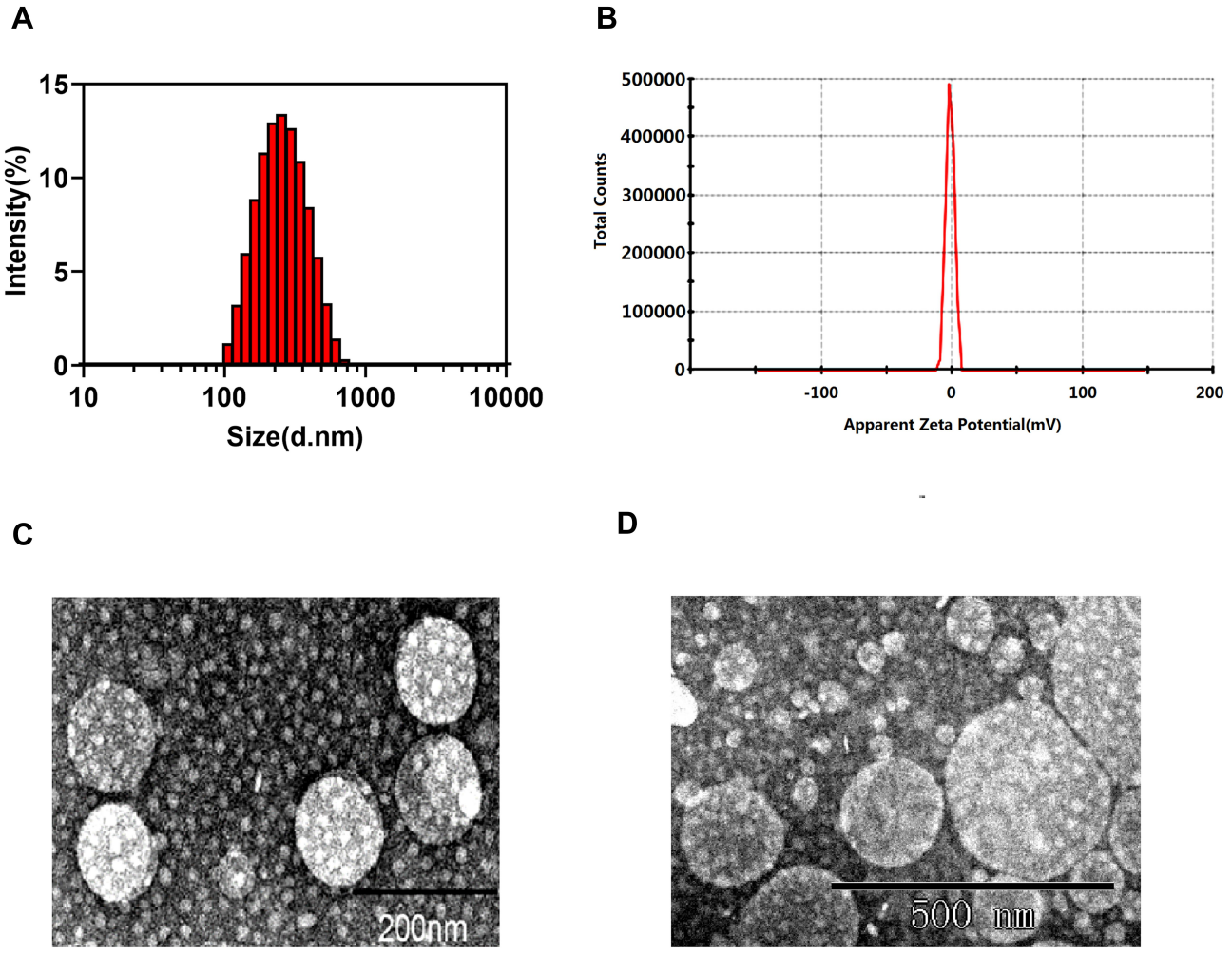

Figure 3 Characterization of TAT-TSL-TMZ/IR820 liposomes. (**A**) Hydrodynamic size distribution in water, (**B**) zeta potential, and (**C** and **D**) TEM image.

undergo tumor aggregation through the EPR effect. The increased vascular permeability of tumor tissues and lymphatic dysfunction (systemic lymph reflux) resulted in EPR, which then resulted in the accumulation of nanoparticles (10–500 nm) at the tumor site. This phenomenon was the passive targeting effect of nanoparticles. The morphological structure of the liposomes was observed via transmission electron microscopy (TEM). The results showed that TAT-TSL-TMZ/IR820 was spherical with a uniform size and without obvious agglomeration. The size measured through TEM was smaller than that measured through DLS likely because of the hydration of the PEG chain of the nanoparticles and the contraction of the nanoparticles caused by the vacuum in TEM.

Second, the UV absorption method was used to determine the TMZ and IR820 contents. The maximum UV absorbance peaks of TMZ and IR820 were approximately 329 and 690 nm, respectively (Figure 4A and B). The standard curves of TMZ and IR820 are shown in Figure 4C and D, respectively. In melanoma cells, IT-CSTNPS acted as the nanometer transfer system in the Core-shell type thermo-nanoparticles loaded with temozolomide combined with photothermal therapy in melanoma cells. The encapsulation rate of TMZ in this nanosystem was 35.4% and and that in IT-CSTNPS was 6.04%. In contrast, nanometer transfer system in this paper is more effective. The vitro drug release experiment performed in this work revealed that the TMZ release rates of the TAT-TSL-TMZ/IR820 liposomes and IT-CSTNPS were 25.47% and 34.1%, respectively, indicating that the nanoparticles prepared in this work had superior stability. Moreover, the nanometer transfer system in this work was more effective than previously reported systems.[25] The loss of excess

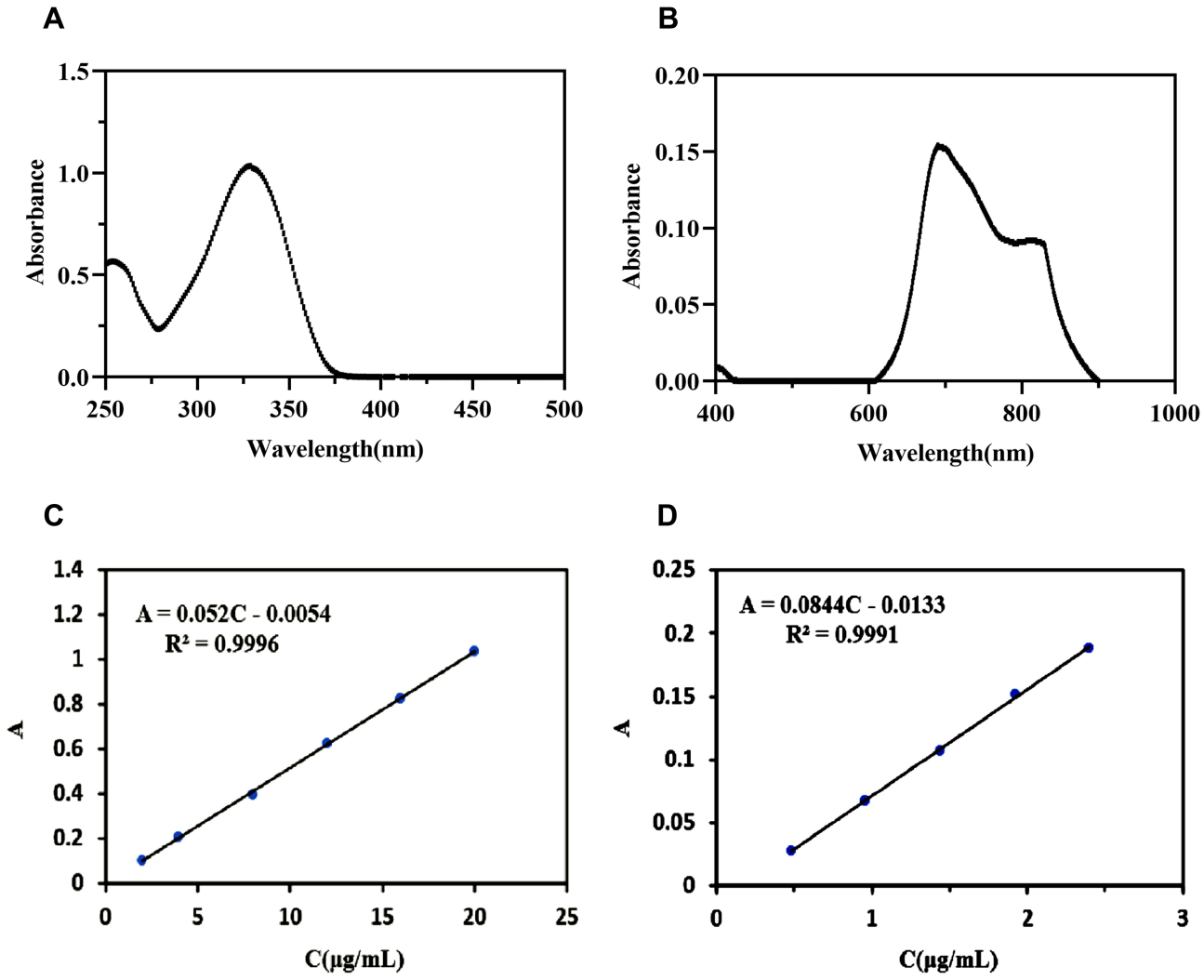

Figure 4 UV absorption spectra of (**A**) TMZ and (**B**) IR820. Standard curves of (**C**) TMZ and (**D**) IR820.

lipids, which could adsorb the drug and form vesicles, during the hydration and extrusion processes of liposome synthesis affected the drug encapsulation rate.

Temperature Increase Curve of TAT-TSL-TMZ/IR820 Liposomes

Temperature changes under laser irradiation were studied in vitro by using an infrared thermal imaging camera to evaluate the photothermal efficiency of TAT-TSL-TMZ /IR820 liposomes. The temperature rise curve collected in this study showed that TAT-TSL-TMZ/IR820 liposomes could reach the maximum temperature within approximately 2 min under laser irradiation at 4 W/cm^2 for 5 min (Figure 5A). The temperature gradually increased with liposome concentration. The temperature difference reached 13.9 °C when the concentration of IR820 in the nanoparticles was 20 μg/mL. By contrast, the temperature in the PBS control group increased only by 2.4 °C and finally reached approximately 27.4 °C when the initial temperature was 25 °C. A temperature difference of 6.8 °C was obtained at the concentration of 10 μg/mL. The maximum temperature could reach 43.8 °C if the

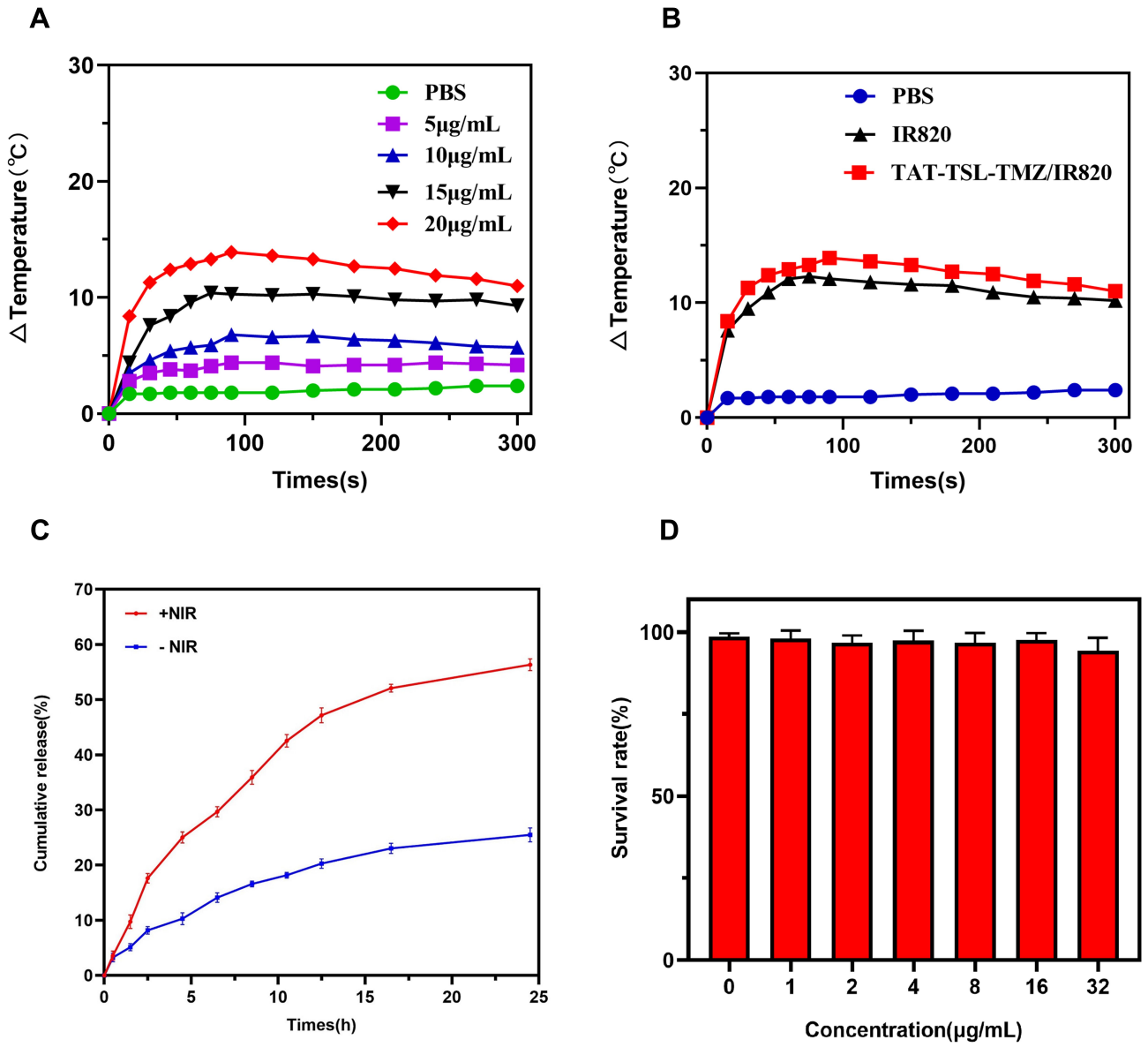

Figure 5 Temperature increase curve measurement. (**A**) Temperature increase curves of different concentrations of TAT-TSL-TMZ/IR820 liposomes (0, 5, 10, 15, and 20 μg/mL) under NIR laser irradiation. (**B**) Temperature increase curves of PBS, IR820 (20 μg/mL), and TAT-TSL-TMZ/IR820 liposomes (20 μg/mL IR820) under NIR laser irradiation. (**C**) In vitro drug release profile of TAT-TSL-TMZ/IR820 liposomes under NIR irradiation. (**D**) The survival rate of MV3 cells after treatment with 0–32 μg/mL TAT-TSL-TMZ/IR820 liposomes for 24 h.

initial temperature was 37 °C. This temperature could increase vascular permeability and drug convection at the disease site and could thus destroy tumor cells without exerting a considerable influence on normal tissues. In addition, TAT-TSL-TMZ/IR820 liposomes had better heating performance under NIR irradiation than free IR820 liposomes (Figure 5B) likely because compared with IR820 nanoparticles, TAT-TSL-TMZ/IR820 liposomes had a higher IR820 concentration and exhibited higher energy efficiency and lower heat dissipation under laser irradiation.

In vitro Drug Release Profile

The TMZ release rate of TAT-TSL-TMZ/IR820 liposomes reached 25.47% within 24 h in the absence of NIR irradiation and 25.03% under 4 h of irradiation (Figure 5C). The total released amount of TMZ reached 56.32% within 24 h after laser irradiation. Thus, NIR irradiation could elevate the solution temperature to the phase transition temperature. This effect induced DPPC to transition from an orderly gelatin state into a disordered liquid crystal state. The liquid crystal state caused the sudden release of the drug by increasing the permeability of the liposome. These results indicated that TAT-TSL-TMZ/IR820 liposomes could release increased amounts of drugs at the high temperatures induced by NIR laser irradiation.

Cytotoxicity of TAT-TSL-TMZ/IR820 Liposomes to MV3 Cells as Determined Through the CCK8 Assay

The biosecurity of nanomaterials is one of the important issues for consideration in the drug development process. The cytotoxicity of TAT-TSL-TMZ/IR820 liposomes to MV3 cells was detected under light-resistant conditions to test the biosecurity of the synthesized drug-loaded liposomes. The experimental results showed that the survival rate of MV3 cells continued to exceed 90% after 24 h of treatment with 0–32 μg/mL TAT-TSL-TMZ/IR820 liposomes (Figure 5D). This result indicated that the synthesized liposomes had good biosecurity.

Cellular Uptake

The cellular uptake of liposomes was observed via fluorescence microscopy and flow cytometry. The fluorescent probe coumarin 6, which was encapsulated in the thermosensitive liposomes, was used to label whole liposomes to track their absorption and intracellular localization. The results of inverted fluorescence microscopy are provided in Figure 6A and showed that the green fluorescence present in MV3 cells was absent from the control group. Green fluorescence was observed in the MV3 cells incubated for 3 h with coumarin 6-labeled TAT-TSL-TMZ/IR820 liposomes. Fluorescence intensity in the MV3 cells was positively correlated with the concentration of TAT-TSL-TMZ/IR820 liposomes. The passage of cell internalization was dependent on concentration within the selected range. Cell uptake was further quantified via flow cytometry. The cell fluorescence signal enhanced with the increase in TAT-TSL-TMZ/IR820 liposomes concentration (Figure 6B). The results of flow cytometry were consistent with those of fluorescence microscopy.

The uptake of TAT-TSL-TMZ/IR820 and TSL-TMZ /IR820 by MV3 cells at the same concentration was investigated to determine the effect of the membrane-penetrating peptide-modified liposomes on cell uptake. As shown in Figure 6C, the fluorescence intensity of the TAT-TSL-TMZ/IR820 group was stronger than that of the TSL-TMZ/IR820 group. Hence, the addition of TAT could accelerate the cellular uptake of liposomes. Flow cytometry also showed that the TAT-TSL-TMZ/IR820 group had a stronger fluorescence signal than the TSL-TMZ/IR820 group (Figure 6D).

Intracellular Localization Profile

As shown in Figure 7, the colocalization of lysosomes and liposomes was observed through CLSM. The yellow area in the merged image represented coumarin 6-labeled liposomes (green fluorescence) that colocalized with lysosomes (red fluorescence). The colocalization of the liposomes with lysosomes indicated that TAT-TSL-TMZ/IR820 liposomes could enter cells via endocytosis and then further enter lysosomes via endocytosis vesicles.

Effects of TAT-TSL-TMZ/IR820 Liposomes on Melanoma MV3 Cells Under NIR Irradiation as Determined by CCK-8 and 513/5000 Killing Effect

The temperature rise curve indicated that TAT-TSL-TMZ /IR820 liposomes had good photothermal conversion performance. The antitumor effect of TAT-TSL-TMZ/IR820 liposomes under NIR irradiation was studied by using the CCK8 method to detect whether the nanoparticles had synergistic chemotherapy and PTT effects. As shown in Figure 8, no significant differences were observed between the cell

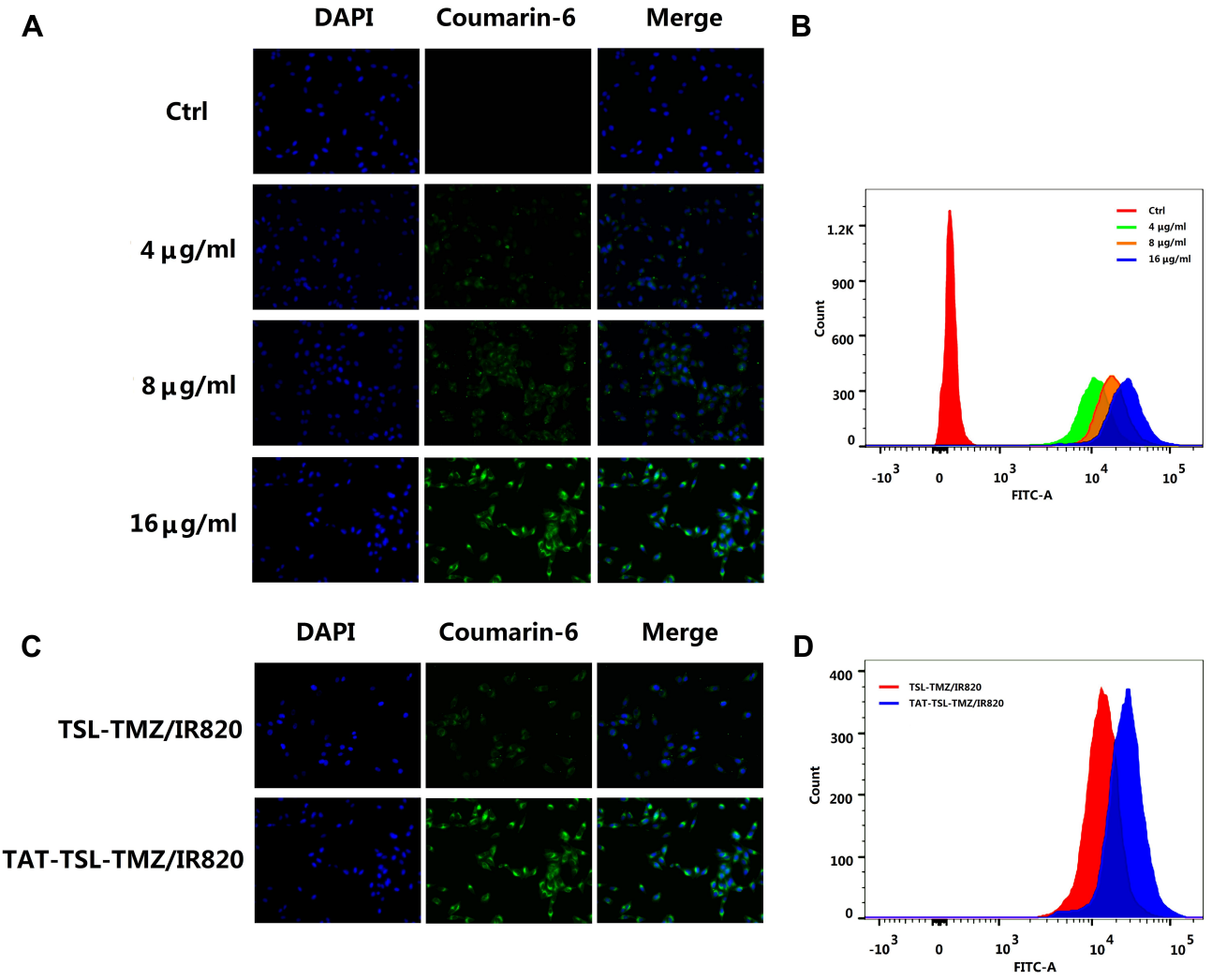

Figure 6 Dose-dependent cellular uptake of TAT-TSL-TMZ/IR820 liposomes by MV3 melanoma cells as measured by (**A**) inverted fluorescence microscopy (magnification, x200) and (**B**) flow cytometry. Cellular uptake of TAT-TSL-TMZ/IR820 and TSL-TMZ/IR820 liposomes of the same concentration as measured by (**C**) inverted fluorescence microscopy (magnification, x200) and (**D**) flow cytometry.
Abbreviation: FITC, fluorescein isothiocyanate.

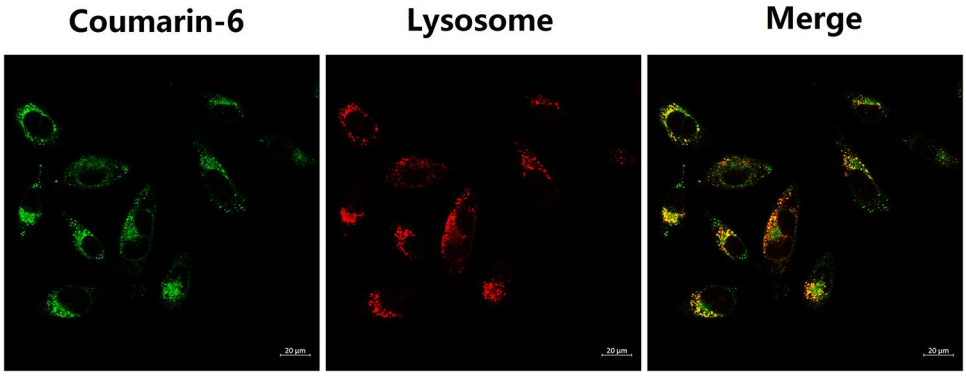

Figure 7 Intracellular localization measurement of TAT-TSL-TMZ/IR820 liposomes in MV3 cells. Scale bar, 20 μm.

survival rates of the NIR and TAT-TSL-TMZ/IR820 groups ($P > 0.05$). Under NIR irradiation, the cell survival rate of the IR820+NIR treatment group decreased slightly to 71.3%. The cell survival rates of the TAT-TSL-TMZ+NIR and TAT-TSL-TR820 +NIR groups were 63.84% and 50.85%, respectively, and were not significantly different

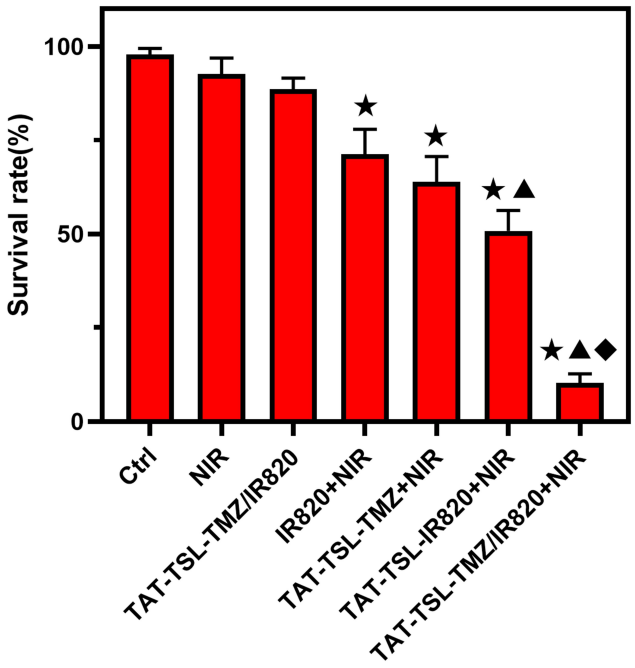

Figure 8 The killing effect of nanoparticles combined with NIR on MV3 cells was detected by CCK8 method. Compared with CTRL group, ★P < 0.05; ▲P < 0.05 compared with IR820+NIR group; ◆P < 0.05 compared with TAT-TSL-TMZ+NIR and TAT-TSL-IR820+NIR groups.

(P > 0.05). Meanwhile, the cell survival rate of the TAT-TSL-IR820+NIR group was statistically significantly different from that of the IR820+NIR group (P < 0.05). The cell survival rate of the TAT-TSL-TMZ/IR820+NIR group significantly decreased to 10.27%, which was significantly lower than that of the TAT-TSL-TMZ+NIR and TAT-TSL-IR820+NIR groups (P < 0.05). These results indicated that TAT-TSL-TMZ/IR820 liposomes had combined chemotherapy and photothermal effects.

Discussion

TMZ is a new second-generation oral alkylating agent with high bioavailability, wide tissue distribution, and the capability to pass through the blood–brain barrier. It exerts a certain therapeutic effect on the brain metastasis of melanoma.[26] This drug has a positive effect in patients with melanoma, especially in those with central system metastasis, and exhibits a 21% effective rate; the low effective rate of chemotherapy in patients with melanoma is related to tumor resistance and affects prognosis.[27] Traditional chemotherapy lacks specificity for tumor cells and can kill tumor cells and normal tissues.

Nanometer drug delivery systems have been applied in tumor treatment. These systems can accumulate at the tumor site to release drugs and reduce toxic and side effects. Moreover, they have good biocompatibility. Although photodynamic therapy (PDT) is a promising minimally invasive approach, traditional photosensitizers are not targeted, poorly soluble, unstable, and easily affected by the internal environment. The combined use of nanotechnology bypasses these limitations and opens up new prospects for the application of PDT in the treatment of different types of diseases. Nanoparticle-mediated PTT has been widely used in NIR irradiation hyperthermia.[28] Gorgizadeh's team[29] studied and synthesized new photothermal nanomaterials, namely, carbon dry gel nanoparticles, and combined the use of these materials with NIR for the treatment of melanoma. In vivo and in vitro experiments showed that their system has considerable antitumor effects. Combination therapy not only enhances therapeutic effects but also avoids the emergence of drug resistance. Thus, combination therapy shows great potential in the treatment of melanoma.

Therefore, we hoped to improve the efficacy of TMZ and reduce side effects by designing a NDDS that could activate or trigger the release of high concentrations of free drugs at the lesion site. We designed and successfully constructed a new nanodrug release system, TI-NP, with a hydration particle size of 167 nm and a charge of −1.37 mV. DLS results verified that the liposomes prepared in this study were TAT-TSL-IR820-TMZ liposomes with uniform particle sizes. TEM results revealed that the liposomes presented a single distribution state, which might facilitate reaching the tumor site through the EPR effect. The EE values of TMZ and IR820 measured via the UV absorption method were 35.4% and 28.6%, respectively. The heating curve indicated that TAT-TSL-TMZ/IR820 liposomes had good heating performance. The adsorption of TAT-TSL-TMZ/IR820 liposomes by MV3 cells exceeded that of TSL-TMZ/IR820 liposomes. This result verified that TATs could well assist liposomes to enter cells through the cell membrane. Laser confocal microscopy illustrated that TAT-TSL-TMZ/IR820 liposomes (green) fused with lysosomes (red) signals, suggesting that liposomes colocalized with lysosomes and that TAT-TSL-TMZ/IR820 liposomes entered cells through endocytosis and concentrated in lysosomes. The experimental results revealed that the survival rate of MV3 cells remained at 90% after 24 h of treatment with 0–32 g/mL TAT-TSL-TMZ/IR820 liposomes (Figure 5D). Therefore, the synthesized liposomes had good biosafety. Our results further indicated that ITNP and TITNP combined with NIR had better antitumor effect than TINP and TTNP alone. The cell activity of the ITNP group decreased slightly (P < 0.05), whereas that of the TITNP group

decreased significantly ($P < 0.05$). Our experiments revealed that combination therapy was more effective than chemotherapy and light therapy alone.

TITNP nanoparticles had good photothermal conversion and drug release performance. They could be ingested in large quantities by melanoma cells and localize in lysosomes after cell entry. CCK-8 experiments demonstrated that TITNP nanoparticles showed better efficacy and safety against MV3 cells under NIR irradiation than the nontargeted treatment (ITNP) and other single chemotherapy or photothermal treatments.

In summary, we successfully designed a new multifunctional nanoliposome drug delivery system that combined PTT and chemotherapy. Through NIR irradiation, TMZ carried by liposomes could be released effectively and localize in cell lysosomes after cell entry. Through continuous in-depth research and exploration, this new targeted drug delivery system might help improve the specificity of chemotherapy drugs for tumor cells and reduce toxicity, side effects, and drug resistance in future clinical practice.

Conclusions

A NIR-triggered TAT-based targeted drug delivery system called TAT-TSL-TMZ/IR820 liposomes was successfully developed. The photothermal conversion capability, cellular uptake, and intracellular localization of this system were investigated. This system is expected to provide new directions for the combined chemo/PTT of melanoma.

Funding

This work was supported by the National Natural Science Foundation of China (No. 81872493, 81803151), the China Post-doctoral Science Foundation (No.2017T100407), the Jiangsu Provincial Medical Talent Foundation the 'SixTalent Peaks' Project of Jiangsu Province (No.WSW-074, WSN-254).

Disclosure

The authors report no conflicts of interest in this work.

References

1. Damsky WE, Bosenberg M. Melanocytic nevi and melanoma: unraveling a complex relationship. *Oncogene*. 2017;36(42):5771–5792.
2. Olbryt M. Molecular background of skin melanoma development and progression: therapeutic implications. *Postepy Dermatol Alergol*. 2019;36(2):129–138. doi:10.5114/ada.2019.84590
3. Rastrelli M, Tropea S, Rossi CR, et al. Melanoma: epidemiology, risk factors, pathogenesis, diagnosis and classification. *In Vivo*. 2014;28(6):1005–1011.
4. Tripp MK, Watson M, Balk SJ, et al. State of the science on prevention and screening to reduce melanoma incidence and mortality: the time is now. *CA Cancer J Clin*. 2016;66(6):460–480. doi:10.3322/caac.21352
5. Yetisgin A, Cetinel S, Zuvin M, et al. Therapeutic Nanoparticles and Their Targeted Delivery Applications. *Molecules*. 2020;25(9):2193. doi:10.3390/molecules25092193
6. Chou Y-P, Lin Y-K, Chen C-H, et al. Recent advances in polymeric nanosystems for treating cutaneous melanoma and its metastasis. *Curr Pharm Des*. 2018;23(35). doi:10.2174/1381612823666170710121348.
7. Zhu Y, Jia H, Duan Q, et al. Photosensitizer-doped and plasma membrane-responsive liposomes for nuclear drug delivery and multidrug resistance reversal. *ACS Appl Mater Interfaces*. 2020;12(33):36882–36894. doi:10.1021/acsami.0c09110
8. Xiong H, Wu Y, Jiang Z, et al. pH-activatable polymeric nanodrugs enhanced tumor chemo/antiangiogenic combination therapy through improving targeting drug release. *J Colloid Interface Sci*. 2020;565:623. doi:10.1016/j.jcis.2019.12.121
9. Li Y, Xiao BX, Dong J, et al. Near-infrared light-responsive nanoparticles for improved anticancer efficacy through synergistic chemo-photothermal therapy. *Pharm Dev Technol*. 2017;23(1):1–9. doi:10.1080/10837450.2017.1312441
10. Hu Z, Fang C, Li B, et al. First-in-human liver-tumour surgery guided by multispectral fluorescence imaging in the visible and near-infrared-I/II windows. *Nat Biomed Eng*. 2020;4(3):259–271. doi:10.1038/s41551-019-0494-0
11. Bhavane R, Starosolski Z, Stupin I, et al. NIR-II fluorescence imaging using indocyanine green nanoparticles. *Sci Rep*. 2018;8(1):14455. doi:10.1038/s41598-018-32754-y
12. Wu B, Wan B, Lu S-T, et al. Near-infrared light-triggered theranostics for tumor-specific enhanced multimodal imaging and photothermal therapy. *Int J Nanomedicine*. 2017;12:4467–4478. doi:10.2147/IJN.S137835
13. Zhang L, Qin Y, Zhang Z, et al. Dual pH/reduction-responsive hybrid polymeric micelles for targeted chemo-photothermal combination therapy. *Acta Biomater*. 2018;75:371–385. doi:10.1016/j.actbio.2018.05.026
14. Li X, Xing L, Hu Y, et al. An RGD-modified hollow silica@Au core/shell nanoplatform for tumor combination therapy. *Acta Biomater*. 2017;62:273–283. doi:10.1016/j.actbio.2017.08.024
15. Chen Q, Liang C, Wang C, et al. An imagable and photothermal "Abraxane-like" nanodrug for combination cancer therapy to treat subcutaneous and metastatic breast tumors. *Adv Mater Weinheim*. 2015;27(5):903–910. doi:10.1002/adma.201404308
16. Zhang R, Cheng K, Antaris AL, et al. Hybrid anisotropic nanostructures for dual-modal cancer imaging and image-guided chemo-thermo therapies. *Biomaterials*. 2016;103:265–277. doi:10.1016/j.biomaterials.2016.06.063
17. Abri Aghdam M, Bagheri R, Mosafer J, et al. Recent advances on thermosensitive and pH-sensitive liposomes employed in controlled release. *J Control Release*. 2019;315:1–22.
18. De Matos MBC, Beztsinna N, Heyder C, et al. Thermosensitive liposomes for triggered release of cytotoxic proteins. *Eur J Pharm Biopharm*. 2018;132:211–221. doi:10.1016/j.ejpb.2018.09.010
19. Jin Y, Liang X, An Y, et al. Microwave-triggered smart drug release from liposomes co-encapsulating doxorubicin and salt for local combined hyperthermia and chemotherapy of cancer. *Bioconjug Chem*. 2016;27(12):2931–2942. doi:10.1021/acs.bioconjchem.6b00603
20. Huang X, Li M, Bruni R, et al. The effect of thermosensitive liposomal formulations on loading and release of high molecular weight biomolecules. *Int J Pharm*. 2017;524(1–2):279–289. doi:10.1016/j.ijpharm.2017.03.090

21. Soliman GM. Nanoparticles as safe and effective delivery systems of antifungal agents: achievements and challenges. *Int J Pharm*. 2017;523(1):15–32. doi:10.1016/j.ijpharm.2017.03.019
22. Turner DC, Moshkelani D, Shemesh CS, et al. Near-infrared image-guided delivery and controlled release using optimized thermosensitive liposomes. *Pharm Res*. 2012;29(8):2092–2103. doi:10.1007/s11095-012-0738-0
23. Wang Y, Wang S, Shi P. Transcriptional transactivator peptide modified lidocaine-loaded nanoparticulate drug delivery system for topical anesthetic therapy. *Drug Deliv*. 2016;23(9):3193–3199. doi:10.3109/10717544.2016.1160459
24. Zhu Y, Cheng L, Cheng L, et al. Folate and TAT peptide co-modified liposomes exhibit receptor-dependent highly efficient intracellular transport of payload in vitro and in vivo. *Pharm Res*. 2014;31(12):3289–3303. doi:10.1007/s11095-014-1418-z
25. Hou X, Pang Y, Li X, et al. Core-shell type thermo-nanoparticles loaded with temozolomide combined with photothermal therapy in melanoma cells. *Oncol Rep*. 2019. doi:10.3892/or.2019.7329
26. Jiang G, Li R, Sun C, et al. Efficacy and safety between temozolomide alone and temozolomide-based double therapy for malignant melanoma: a meta-analysis. *Tumor Biol*. 2013;35(1):315–322. doi:10.1007/s13277-013-1042-2
27. Bepler G, Begum M, Simon G. Molecular analysis-based treatment strategies for non–small cell lung cancer. *Cancer Control*. 2008;15(2):130–139. doi:10.1177/107327480801500205
28. Fu G, Sanjay S, Dou M, et al. Nanoparticle-mediated photothermal effect enables a new method for quantitative biochemical analysis using a thermometer. *Nanoscale*. 2016;8(10):5422–5427. doi:10.1039/C5NR09051B
29. Gorgizadeh M, Azarpira N, Dehdari Veis R, et al. Repression of melanoma tumor in vitro and in vivo by photothermal effect of carbon xerogel nanoparticles. *Colloids Surf B Biointerfaces*. 2019;176:449–455. doi:10.1016/j.colsurfb.2019.01.032